PRAMANA — journal of physics

Vol. 82, No. 6
June 2014
pp. 1085–1101

A theoretical study of pump–probe experiment in single-layer, bilayer and multilayer graphene

ENAMULLAH*, VIPIN KUMAR, UPENDRA KUMAR and GIRISH S SETLUR

Department of Physics, Indian Institute of Technology Guwahati, Guwahati 781 039, India
*Corresponding author. E-mail: enamullah@iitg.ernet.in

MS received 30 May 2013; revised 10 December 2013; accepted 8 January 2014
DOI: 10.1007/s12043-014-0756-z; ***e*Publication:** 3 June 2014

Abstract. The pump–probe experiment is typically used to study relaxation phenomena in nonlinear optical systems. Here we use it as a tool to study the phenomenon of anomalous Rabi oscillations in graphene that was predicted recently in single-layer graphene. Unlike conventional Rabi oscillations, anomalous Rabi oscillations are unique to graphene (and possibly to surface states of topological insulators (TIs)), attributable to the pseudospin (conventional spin for TI) degree of freedom and Dirac-fermion character of the graphene system. A pump pulse of a finite duration long enough to contain a large number of cycles induces a current density that oscillates with the frequency of the pump pulse. The amplitude associated with these fast oscillations is seen to exhibit much slower oscillations with a frequency given by $2\omega_R^2/\omega$ – the anomalous Rabi frequency, where ω_R is the conventional Rabi frequency and ω is the frequency of the external pump field. This effect is easily probed by a probe pulse subsequent to the pump, where it manifests itself as periodic oscillations of the probe susceptibility as a function of pump duration at each probe frequency. Alternatively, it is also seen as an oscillatory function of the pump–probe delay with other variables remaining fixed. This period corresponds to the anomalous Rabi frequency. An analysis of the previously reported experimental data confirms the presence of anomalous Rabi oscillations in graphene.

Keywords. Graphene; Rabi oscillation; pump–probe experiment.

PACS No. 72.80.Vp

1. Introduction

Graphene is a single layer [1–3] of graphite material made of carbon atoms arranged in a honeycomb crystal lattice with zero band gap and with a linear dispersion relation between energy and momentum for both electrons and holes. Bilayer graphene consists of two graphene layers weakly coupled by Van der Waals force and the low energy spectrum of the Hamiltonian is parabolic, which describes chiral quasiparticles [4,5]. We wish to

study the recently predicted anomalous Rabi oscillations [6] in graphene using the pump–probe method. The phenomenon of conventional Rabi oscillations can be most easily understood in two-level systems [7–9]. Typically, incoherent optical properties such as optical dephasing and relaxation of band electrons in semiconductors are studied using the pump–probe experiment [8,9] in which two successive laser pulses are used, one to prepare the system in a certain way, called pump pulse, and the other to test it after a variable time delay, called probe pulse. Coherent optical response, e.g., the excitonic optical Stark effect of a semiconductor [10–12] is studied by the pump–probe technique in which the pump pulse excites the material energetically below the exciton resonance and the probe pulse monitors the transmission change at exciton resonance. So it is appropriate to investigate such nonlinear properties in two-dimensional single-layer graphene (SLG), bilayer graphene (BLG) and multilayer graphene (MLG) where the bands are linear in the case of SLG and parabolic in the case of BLG, but all of them possess a property unique to these systems, viz. pseudospin.

2. Experimental literature review on the relaxation dynamics in graphene

Recently, many experiments on the relaxation of the carrier dynamics of graphene on different substrates have been performed [13–16]. Some of the experimental results are summarized as follows.

The ultrafast relaxation of photogenerated carriers in epitaxially grown graphene layers on SiC substrate [17] depends on the intraband carrier–carrier and intraband carrier–phonon scattering. The plot between the differential transmission coefficient $((T - T_0)/T_0)$, where, T and T_0 are the probe transmission coefficients with and without pump field respectively, vs. time duration between pump and probe pulse shows two types of relaxations (τ_1) and (τ_2) with different pump pulse energy and temperature. The range of fast relaxation time (τ_1) is nearly 70–120 fs and the range of slow relaxation time (τ_2) is 0.4–1.2 ps. Fast relaxation (τ_1) due to the intraband carrier–carrier scattering leads to the quaisequilibrium states followed by Fermi–Dirac distribution, which is consistent with the theoretically predicted intraband carrier–carrier relaxation in graphene [18]. The slower time delay (τ_2) is attributed to further thermalization such as intraband carrier–phonon scattering.

The experimental plot between the differential transmission coefficient $((T - T_0)/T_0)$ and delay time between pump and probe pulses of carrier relaxation in graphene on mica substrate using femtosecond laser [18] is almost the same as earlier experiments [17] barring some intermittent discrepancies in sign. The plot shows that the initial increase (almost linear) in differential transmission coefficient is due to Pauli blocking or due to the repulsion by the initially generated electron–hole density on further generated photoelectrons. The subsequent decrease in transmission coefficient is due to intraband carrier–carrier and intraband carrier–phonon scatterings. One conclusion of this experiment is that carrier relaxation in graphene is almost the same as that of graphite. This means coupling between different graphite layers plays a minor role in ultrafast carrier relaxation.

Other experiments such as the one performed by Kumar *et al* [19] and on the graphene analogue boron carbon nitrate (BCN) [20] regarding relaxation dynamics of carriers in graphene using femtosecond lasers also shows the two types of relaxation, fast relaxation

τ_1 in the 130–330 fs range and slow relaxation τ_2 in the 3.5–4.9 ps range. Fast relaxation is related to the carrier–carrier scattering, while slow relaxation is related to the carrier–phonon scattering.

Wang *et al* [21] studied the relaxation dynamics of hot optical phonons in few-layers and multilayer graphene grown on silicon carbide substrate and found that the optical phonon cooling rates are very short and independent of factors such as growth technique, number of graphene layers and type of substrate. Time-resolved terahertz spectroscopy is a powerful tool in the investigation of carrier dynamics in semiconductors [22]. The work on multilayer graphene nanostructures [23,24] are particularly relevant for applications in optoelectronics.

The experiments performed by the above groups, especially by Dawlaty *et al* [17], Kumar *et al* [19,20], Breusing *et al* [18] and Wang *et al* [21] are particularly relevant as they appear to confirm the predictions of the present work.

In this article, the recently predicted anomalous Rabi oscillations [6] are studied theoretically by the pump–probe technique where we calculate probe susceptibility for the system of interest as a function of the area of the pump pulse. Anomalous Rabi oscillations manifest themselves as periodic oscillations of the probe susceptibility as a function of pump duration at each probe frequency. The period associated with these oscillations corresponds to the anomalous Rabi frequency. It has been estimated by the authors cited that a quasiequilibrium state due to Coulomb scattering is reached in graphene in a time-scale of $\sim$100 –250 fs and phonon-assisted energy relaxation takes place in a time-scale of 1–2 ps. This means that the phenomena of the present work are seen clearly when a sufficient number of oscillations fit into a time-scale of the order of 250 fs. This in turn translates into a constraint on the peak electric field of the pulses used. More detailed numerical estimates will be provided in §5.

3. Coherent Bloch equations in the presence of intense optical pump field

In what follows, we describe the effect of a finite duration pump pulse on the time evolution of the polarization and densities of charge carriers in graphene. This has been done in detail in our earlier work [6]; hence, we shall be content at reproducing only the salient features. Upon extinguishing the pump pulse, the dynamical quantities in the system temporarily freeze to a value determined by the so-called area of the pulse [8]. These then serve as background for the probe pulse that follows immediately afterward (this assumption makes the analysis simpler). The idea is that a study of the probe susceptibility as a function of the pump pulse duration can extract the anomalous Rabi frequency – a characteristic unique to the graphene systems as we have already pointed out.

3.1 *Bloch equations for single-layer graphene*

The Hamiltonian for the low-energy spectrum of graphene in the presence of an intense optical pump field can be written into the second quantization language as

$$H = \sum_{p,\alpha,\beta} v_{\mathrm{F}} \vec{\sigma}_{\alpha,\beta} \cdot \left(\vec{p} - \frac{e}{c}\vec{A}(t)\right) c^{\dagger}_{p,\alpha} c_{p,\beta},$$

where the Greek indices stand for either sublattice A or sublattice B of the honeycomb crystal lattice and $c^{\dagger}(c)$ is the creation(annihilation) operator, σ are the three sets of Pauli matrices, p is the momentum of fermions, $\vec{A}(t) = \vec{A}(0)\mathrm{e}^{-i\omega t}$ is the complex vector potential corresponding to the pump field. With the help of Heisenberg's equation of motion we have derived the equation of motion for the elements of reduced density matrix

$$n_{\mathrm{diff}}(\vec{k},t) = n_{\mathrm{A}}(\vec{k},t) - n_{\mathrm{B}}(\vec{k},t) = \langle c^{\dagger}_{k,\mathrm{A}}(t)c_{k,\mathrm{A}}(t)\rangle - \langle c^{\dagger}_{k,\mathrm{B}}(t)c_{k,\mathrm{B}}(t)\rangle$$

and

$$\langle c^{\dagger}_{k,\mathrm{A}}(t)c_{k,\mathrm{B}}(t)\rangle = p(\vec{k},t).$$

The optical Bloch equation without Coulomb interaction derived in our earlier study [6] is given by (since it is necessary to write here)

$$\frac{\partial}{\partial t}n_{\mathrm{diff}}(\vec{k},t) = 4\ \mathrm{Im}\left[v_{\mathrm{F}}\vec{\sigma}_{\mathrm{AB}}\cdot\left(\vec{k}-\frac{e}{c}\vec{A}^{*}(t)\right)p(\vec{k},t)\right]$$

$$i\frac{\partial}{\partial t}p(\vec{k},t) = v_{\mathrm{F}}\vec{\sigma}_{\mathrm{BA}}\cdot\left(\vec{k}-\frac{e}{c}\vec{A}(t)\right)n_{\mathrm{diff}}(\vec{k},t).$$

These Bloch equations may be solved using an alternative to the well-known rotating wave approximation (RWA), which have been called asymptotic RWA (ARWA) [6]. In this approximation, quantities such as number density and polarization are expressed as a harmonic series involving the largest of the frequencies and the coefficients are assumed to be slowly varying on the scale of this frequency. In the ARWA regime, this large frequency is ω, the pump frequency. A detailed justification for the use of this approximation is given in our earlier work [6]. Following our earlier work, we decompose the pump pulse polarization and population excess as follows:

$$p(\vec{k},t) = p_s(\vec{k},t) + p_+(\vec{k},t)\mathrm{e}^{-i\omega t} + p_-(\vec{k},t)\mathrm{e}^{i\omega t}$$

and

$$n_{\mathrm{diff}}(\vec{k},t) = n_s(\vec{k},t) + n_f(\vec{k},t)\mathrm{e}^{-i\omega t} + n^{*}_f(\vec{k},t)\mathrm{e}^{i\omega t}.$$

The pump solution has been found in our earlier work as follows:

$$p_+(\vec{k},t) \approx -\frac{z_{\mathrm{R}}(t)}{\omega}n_s(\vec{k},t);\ \ n_f(\vec{k},t) \approx \frac{2z_{\mathrm{R}}(t)}{\omega}\ p^{*}_s(\vec{k},t)$$

and

$$p_-(\vec{k},t) \approx -\frac{2z^{*}_{\mathrm{R}}(t)z^{*}_k}{\omega^2}\ p_s(\vec{k},t)$$

and

$$p_s(\vec{k},t \le T_i) = -\frac{k_x + ik_y}{2|k|} = -\frac{z^{*}_k}{2v_{\mathrm{F}}|k|}\ ;\ n_s(\vec{k},t \le T_i) = 0,$$

where we take the pump pulse field to be in the interval $T_i < t < T_f$. The expression for slowly varying part is

$$\partial_t n_s(\vec{k},t) = 4\ \mathrm{Im}[z_k p_s(\vec{k},t)], \qquad i\,\partial_t p_s(\vec{k},t) = z^{*}_k\ n_s(\vec{k},t) - \frac{2\omega^2_{\mathrm{R}}(t)}{\omega}\ p_s(\vec{k},t)$$

and the expression for generalized anomalous Rabi frequency

$$\Omega_{\mathrm{AR}}(\vec{k},t)=\sqrt{4(v_{\mathrm{F}}|k|)^2+\left(\frac{2\omega_{\mathrm{R}}^2(t)}{\omega}\right)^2},$$

$$n_s(\vec{k},t\geq T_i)=n_s(\vec{k},T_i)\cos(\Phi(t)),\qquad n_s(\vec{k},T_i)=\frac{\omega(v_{\mathrm{F}}|k|)}{\omega_{\mathrm{R}}^2(\bar{t})},$$

$$p_s(\vec{k},t\geq T_i)=\frac{\Omega_{\mathrm{R}}(\bar{t})z_k^*\omega}{4i(v_{\mathrm{F}}|k|)\omega_{\mathrm{R}}^2(\bar{t})}\left(\sin(\Phi(t))-i\,\frac{2\omega_{\mathrm{R}}^2(\bar{t})}{\omega\Omega_{\mathrm{R}}(\bar{t})}\cos(\Phi(t))\right),$$

where the quantity $\Phi(\vec{k},t)=\int_{T_i}^{t}\Omega_{\mathrm{R}}(\vec{k},t')\,\mathrm{d}t'$ is called 'the area of the pulse'. The quantity

$$\omega_{\mathrm{R}}^2(t)=z_{\mathrm{R}}^*(t)z_{\mathrm{R}}(t)=\left|v_{\mathrm{F}}\frac{e}{c}(\vec{\sigma}_{\mathrm{BA}}\cdot\vec{A}_s(t))\right|^2$$

is the square of the conventional Rabi frequency at zero detuning, changing adiabatically in time as a function of the pump envelope field. Also,

$$\omega_{\mathrm{R}}^2(\bar{t})=\frac{\int_{T_i}^{t}\mathrm{d}t'\;\omega_{\mathrm{R}}^2(t')}{(t-T_i)}$$

is the time average of the square of the conventional Rabi frequency. For the purposes of the present work, we choose the shape of the slowly varying part of the vector potential $\vec{A}_s(t)$ as

$$\vec{A}_s(t)=\frac{\sqrt{2}\vec{A}(0)}{\sqrt{T_f-T_i}}(t-T_i)^{1/2}\Theta\left(\frac{T_i+T_f}{2}-t\right)\Theta(T_f-t)$$
$$+\frac{\sqrt{2}\vec{A}(0)}{\sqrt{T_f-T_i}}(T_f-t)^{1/2}\Theta\left(t-\frac{T_i+T_f}{2}\right)\Theta(T_f-t).$$

The precise shape, of course, does not matter since the basic physics we seek is to establish the phenomenon of anomalous Rabi oscillations. The expression for the area of pulse becomes

$$\phi(k)=\sqrt{16(v_{\mathrm{F}}|k|)^2+(T_f-T_i)^2Z^2},$$

$$\Phi(\vec{k},t\geq T_f)=\frac{1}{4}(T_f-T_i)\phi(k)+\frac{2(v_{\mathrm{F}}|k|)^2}{Z}$$
$$\times\log\left(\frac{(T_f-T_i)Z+\phi(k)}{-(T_f-T_i)Z+\phi(k)}\right)+2v_{\mathrm{F}}|k|(t-T_f),$$

where

$$Z=\frac{4|z_{\max}|^2}{\omega(T_f-T_i)}.$$

In the discussion that follows, we assume that the probe pulse is immediately applied upon extinguishing the pump pulse and the former is of such a short duration that it is legitimate to use a delta function probe. The main reason for this assumption is that we want only the anomalous Rabi frequency to contribute to the area of the pulse and not the free particle dispersion (even if k is small $2v_F|k|(t_{pr} - T_f)$ may not be small if $t_{pr} \gg T_f$). In this case, the time average of Rabi frequency and generalized Rabi frequencies become

$$\omega_R^2(\bar{t}) = \frac{\int_{T_i}^{T_f} dt'\, \omega_R^2(t')}{(T_f - T_i)} = \frac{|z_{max}|^2}{2}$$

$$\Omega_{AR}(\vec{k}, \bar{t}) = \sqrt{4(v_F|k|)^2 + \frac{|z_{max}|^4}{\omega^2}}$$

and the area of the pulse may be simply written as

$$\Phi(t_{pr}) = (T_f - T_i)\frac{|z_{max}|^2}{\omega} = (T_f - T_i)\frac{2\omega_R^2(\bar{t})}{\omega}.$$

In passing, we note that the Bloch equations are a special case of what is known as the Floquet equation [25] in mathematics. This formalism has also been used extensively in the physics literature especially in the field of atomic physics where atom–light interactions are studied [26]. The Rabi frequency that we deduce (both anomalous and conventional) are known as Floquet exponents. In this sense, there is nothing mysterious about the anomalous Rabi frequency or indeed the conventional one. However, the point in focus is that these exponents vanish in some regime for peudospinless systems, whereas they do not when there is pseudospin (hence the adjective 'anomalous'). In the present situation, according to that theory, there are three Floquet exponents that add up to zero. Since they are symmetrically placed, one of them is zero and the other two are equal and opposite in sign. This is the Rabi frequency. However, this theory does not provide a simple analytical expression for these coefficients and, in most situations, they have to be obtained numerically if the exact answer is needed. Hence, our analytical approach, though approximate unlike the numerical approach, is needed to establish the general relationships between the Rabi frequency and models under study and regimes considered.

Now we go on to derive Bloch equations for the pump and probe pulses in the case of bilayer and multilayer graphene specifically tailored to probe anomalous Rabi oscillations.

3.2 *Bloch equations for bilayer graphene*

The low-energy properties of BLG with Bernal stacking are well described by an off-diagonal Hamiltonian with parabolic dispersion [4,5]. The Hamiltonian for BLG in the presence of an optical pump field is given by

$$\hat{H} = -\frac{1}{2m}\sum_p \left(p_x - ip_y - \frac{e}{c}A^*(t)\right)^2 c_{A1}^\dagger(\vec{p})c_{B2}(\vec{p}) + \text{h.c.},$$

where $m = \gamma_1/2v_F^2$ is the effective mass of Dirac fermions, related to the interlayer hopping parameter γ_1 and Fermi velocity v_F.

We may now find the equation of motion for the reduced density matrix with elements,

$$n_{\rm diff}(\vec{k},t) = n_{\rm A1}(\vec{k},t) - n_{\rm B2}(\vec{k},t) = \langle c^{\dagger}_{k,{\rm A1}}(t)c_{k,{\rm A1}}(t)\rangle - \langle c^{\dagger}_{k,{\rm B2}}(t)c_{k,{\rm B2}}(t)\rangle$$

and

$$p(\vec{k},t) = \langle c^{\dagger}_{k,{\rm A1}}(t)c_{k,{\rm B2}}(t)\rangle$$

as follows:

$$\frac{\partial}{\partial t}n_{\rm diff}(\vec{k},t) = -\frac{2}{m}{\rm Im}\left[\left(k_x - ik_y - \frac{e}{c}A^*(t)\right)^2 p(\vec{k},t)\right]$$

$$i\frac{\partial}{\partial t}p(\vec{k},t) = -\frac{1}{2m}\left(k_x + ik_y - \frac{e}{c}A(t)\right)^2 n_{\rm diff}(\vec{k},t).$$

In the ARWA method [6], these are solved using the ansatzs,

$$\begin{aligned} n_{\rm diff}(\vec{k},t) &= n_s(\vec{k},t) + n_f(\vec{k},t){\rm e}^{-i\omega t} + n^*_f(\vec{k},t){\rm e}^{i\omega t} \\ &\quad + n'_f(\vec{k},t){\rm e}^{-2i\omega t} + n'^*_f(\vec{k},t){\rm e}^{2i\omega t}, \\ p(\vec{k},t) &= p_s(\vec{k},t) + p_+(\vec{k},t){\rm e}^{-i\omega t} + p_-(\vec{k},t){\rm e}^{i\omega t} \\ &\quad + p'_+(\vec{k},t){\rm e}^{-2i\omega t} + p'_-(\vec{k},t){\rm e}^{2i\omega t}. \end{aligned}$$

For two layers it is important to include terms upto the second harmonic at least. This becomes clear if we focus on the $k = 0$ case where anomalous Rabi oscillations are seen at the level of the second harmonic and are absent at the level of the first harmonic. This idea will be made more general when we discuss multilayer graphene in the next section. Upon substitution in the Bloch equations, the solutions for rapidly varying parts of the above Bloch equations are given by

$$\begin{aligned} n_f(\vec{k},t) &\approx \frac{4\alpha(e/c)k_+A_s(t)}{\omega}p^*_s(\vec{k},t), \quad n'_f(\vec{k},t) \approx -\frac{2\alpha(e/c)^2A^2_s(t)}{2\omega}p^*_s(\vec{k},t) \\ p_-(\vec{k},t) &\approx -\frac{2\alpha^2}{\omega^2}\left(2(e/c)|k|^2 + (e/c)^3|A_s(t)|^2\right) \\ &\quad \times k_+A^*_s(t)p_s(\vec{k},t) \\ p_+(\vec{k},t) &\approx -\frac{2\alpha(e/c)k_+A_s(t)}{\omega}n_s(\vec{k},t), \quad p'_+(\vec{k},t) \approx \frac{\alpha(e/c)^2A^2_s(t)}{2\omega}n_s(\vec{k},t) \\ p'_-(\vec{k},t) &\approx \frac{2\alpha^2(e/c)^2k^2_+A^{*2}_s(t)}{4\omega^2}p_s(\vec{k},t), \end{aligned}$$

where $k_\pm = k_x \pm ik_y$. We may see from the above expression that unlike in the single-layer case, in bilayer when $k = 0$, the contribution from the first harmonic completely drops out. This is because $p_\pm(\mathbf{0},t) \equiv 0$ and $n_f(\mathbf{0},t) \equiv 0$. Therefore, anomalous Rabi oscillations in the bilayer case are seen only at the level of the second harmonic for small values of k. The solutions for the slowly varying parts are given by

$$n_s(\vec{k},t \geq T_i) = n_s(\vec{k},T_i)\cos(\Phi(t)) = \frac{\omega|k|^2}{2m\omega^2_{\rm R}(\bar{t})}\cos(\Phi(t))$$

$$p_s(\vec{k}, t \geq T_i) = \frac{k_+^2}{2|k|^2}\left(\cos(\Phi(t)) + i\frac{\omega\Omega_{\rm AR}(\bar{t})}{\omega_{\rm R}^2(\bar{t})}\sin(\Phi(t))\right).$$

We may neglect $p_-(\vec{k}, t)$ and $p'_-(\vec{k}, t)$ as they are smaller than the included terms by at least two factors of $1/\omega$. The important ingredient that enters into these equations is $\Phi(t)$ – the area of the pulse given by the following expression (in which we use the same shape of $A_s(t)$ as in the case of single layer):

$$\Phi(t \geq T_f) = \frac{1}{3\omega}\left(\frac{1}{2m}\right)^2 \left(\frac{e}{c}\right)^4 |A(0)|^4\ (T_f - T_i) + \frac{k^2}{m}(t - T_f).$$

The above expression is derived by assuming small values of band momentum k. This analysis also yields an expression for the anomalous Rabi frequency,

$$\Omega_{\rm AR}^{\rm BLG}(t) = \sqrt{\left(\frac{|k|^2}{2m}\right)^2 + \frac{\left(2\omega_{\rm R}^2(t) + 4\sqrt{2}\frac{|k|^2\omega_{\rm R}(t)}{m}\right)^2}{4\omega^2}},$$

where

$$\omega_{\rm R}^2(t) \approx \left(\frac{1}{2m}\right)^2 \frac{(e/c)^4|A_s(t)|^4}{2}$$

is the conventional Rabi frequency.

Now we go on to generalize this to n-layers. The discussion is quite similar. However in the general case, one must treat higher harmonics with care.

3.3 *Bloch equations for multilayer graphene*

The Hamiltonian for MLG [27] in the presence of an optical pump field may be modelled as

$$\hat{H}_n = \sum_p \sum_{j=1}^{n-1} \left(p_- - \frac{e}{c}A^*(t)\right)^n c_{{\rm A}j}^\dagger(\vec{p}, t)\ c_{{\rm B}(j+1)}(\vec{p}, t) + \text{h.c.},$$

where $\beta = v_{\rm F}^n/\gamma_1^{n-1}$, $p_\pm = p_x \pm ip_y$. With the help of Heisenberg's equation we can find the equation of motion for the following elements of reduced density matrix:

$$N_\nu(\vec{k}, t) = \langle c_{{\rm A}\nu}^\dagger(\vec{k}, t)c_{{\rm A}\nu}(\vec{k}, t)\rangle - \langle c_{{\rm B}(\nu+1)}^\dagger(\vec{k}, t)c_{{\rm B}(\nu+1)}(\vec{k}, t)\rangle$$

and

$$\pi_\nu(\vec{k}, t) = \langle c_{{\rm A}(\nu)}^\dagger(\vec{k}, t)c_{{\rm B}(\nu+1)}(\vec{k}, t)\rangle$$

for the νth layer as

$$i\frac{\partial}{\partial t}N_\nu(\vec{k}, t) = 4\beta\ {\rm Im}\left[\left(k_-^n - n\ \frac{e}{c}\ A^*(t)k_-^{n-1}\right)\pi_\nu(\vec{k}, t)\right]$$

$$i\frac{\partial}{\partial t}\pi_\nu(\vec{k}, t) = \beta\left(k_+^n - n\ \frac{e}{c}\ A(t)k_+^{n-1}\right)N_\nu(\vec{k}, t).$$

Using the ARWA technique [6], we make the following substitution (keeping in mind that at $k = 0$, the polarization varies slowly, whereas the population oscillates with frequency equal to the nth harmonic in the external frequency):

$$\pi_v(\vec{k}, t) = \pi_s(\vec{k}, t) + \mathrm{e}^{-i\omega t}\pi_+(\vec{k}, t) + \mathrm{e}^{i\omega t}\pi_-(\vec{k}, t)$$

$$N_v(\vec{k}, t) = \mathrm{e}^{in\omega t}N_{\max}(\vec{k}, t) + \mathrm{e}^{-in\omega t}N^*_{\max}(\vec{k}, t) + \mathrm{e}^{i(n-1)\omega t}N_{\max,1}(\vec{k}, t) + \mathrm{e}^{-i(n-1)\omega t}N^*_{\max,1}(\vec{k}, t).$$

After substituting these values in the above Bloch equation and comparing the coefficients we have

$$N_{\max}(\vec{k}, t) = -\frac{2\beta(-\frac{e}{c}A^*_s(t))^n}{n\omega}\pi_s(\vec{k}, t);$$

$$N_{\max,1}(\vec{k}, t) = -\frac{2n\beta(-\frac{e}{c}A^*_s(t))^{(n-1)}p_-}{(n-1)\omega}\pi_s(\vec{k}, t);$$

$$\pi_-(\vec{k}, t) = \frac{2\beta^2(-\frac{e}{c}A_s(t))^{(n-1)}(-\frac{e}{c}A^*_s(t))^n p_+}{\omega^2}\pi_s(\vec{k}, t);$$

$$\pi_+(\vec{k}, t) = -\frac{2n^2\beta^2(-\frac{e}{c}A_s(t))^n\ (-\frac{e}{c}A^*_s(t))^{(n-1)}p_-}{(n-1)\omega^2}\pi_s(\vec{k}, t),$$

and the equation for the slowly varying part of the polarization is $(\partial/\partial t)\pi_s(\vec{k}, t) = i\Omega_{\mathrm{R}}^{\mathrm{NLG}}(t)\pi_s(\vec{k}, t)$ where $\Omega_{\mathrm{R}}^{\mathrm{NLG}}(t)$ is the generalized Rabi frequency given by the following expression:

$$\Omega_{\mathrm{R}}^{\mathrm{NLG}}(t) = \frac{2\beta^2|-\frac{e}{c}A_s(t)|^{2n}}{n\omega} + \frac{2n^2\beta^2|k|^2\ |-\frac{e}{c}A_s(t)|^{2(n-1)}}{\omega(n-1)}$$

and the solution for $\pi_s(\vec{k}, t)$ is given by

$$\pi_s(\vec{k}, t) = \pi_s(\vec{k}, 0)\,(\cos(\Phi(t)) + i\,\sin(\Phi(t)))\,,$$

where

$$\pi_s(\vec{k}, 0) = (-1)^n\frac{k_+^n}{2|k|^n}$$

can be found by the equilibrium condition and $\Phi(t)$, the area of the pulse with the same shape of $A_s(t)$ taken in the case of both single layer and bilayer is given by

$$\Phi(t) = \frac{2\beta^2}{n(n+1)\omega}\ \left(\frac{e}{c}\right)^{2n}|A(0)|^{2n}\ (T_f - T_i) + \beta|k|^n(t - T_f).$$

The above expression is derived assuming small 'k' values. The area of the pulse assumes this value just at the end of the pump pulse when the pump is tuned off. If the probe is incident at this time, the dynamics of the probe is determined by the above area of the pump pulse.

So far we have described the influence of the pump pulse field on the dynamics of single layer, bilayer and multilayer graphene. Now we go on to describe the effect of a weak probe pulse on the graphene systems excited by the pump field as described above.

4. Linear response equations of the probe field

The probe field being weak, obeys linearized Bloch equations. To linearize the Bloch equations, we write

$$n_{\rm diff}(\vec{k},t) \to n_{\rm diff}(\vec{k},t) + \delta n_{\rm diff}(\vec{k},t), \qquad p(\vec{k},t) \to p(\vec{k},t) + \delta p(\vec{k},t).$$

Here $\delta n_{\rm diff}(\vec{k},t)$, $\delta p(\vec{k},t)$ and $\delta p^*(\vec{k},t)$ are the linear response functions due to the probe field.

4.1 *Linear response of a single layer*

After linearizing the Bloch equations for single layer we have

$$\frac{\rm d}{{\rm d}t}\delta n_{\rm diff}(\vec{k},t) = 4\ {\rm Im}[z_k \delta p(\vec{k},t) + \delta z_{\rm A}(t) p_s^*(\vec{k},t)]$$
$$i\frac{\rm d}{{\rm d}t}\delta p(\vec{k},t) = z_k^*\ \delta n_{\rm diff}(\vec{k},t) - \delta z_{\rm A}(t) n_s(\vec{k},t).$$

We solve these coupled equations with initial condition $\delta n_{\rm diff}(\vec{k},t_{\rm pr}) = 0$ and $\delta p(\vec{k},t_{\rm pr}) = 0$ at time $t = t_{\rm pr}$ just before the probe field assumed to be a delta function at $t = t_{\rm pr}$. In other words, we set $\delta z_{\rm A}(t') = (\delta z_{\rm A,max} t_{\rm pr})\delta(t' - t_{\rm pr})$. After solving these equations, we get the following expressions for $\delta n_{\rm diff}(\vec{k},t)$ and $\delta p(\vec{k},t)$:

$$\delta n_{\rm diff}(\vec{k},t) = -i\,Q(t_{\rm pr})\Theta(t - t_{\rm pr})\cos(2|z_k|(t - t_{\rm pr})) + \frac{n_s(t_{\rm pr})}{|z_k|} 2\ {\rm Re}[z_k \delta A(t_{\rm pr})]\Theta(t - t_{\rm pr})\cos(2|z_k|(t - t_{\rm pr}))$$

and

$$\begin{aligned}\delta p(\vec{k},t) \ =\ & -\frac{n_s(\vec{k},t_{\rm pr})}{z_k}\ {\rm Im}[z_k(\delta z_{\rm A,max} t_{\rm pr})]\Theta(t - t_{\rm pr}) \\ & + \frac{i\ n_s(\vec{k},t_{\rm pr})}{z_k}\ {\rm Re}[z_k \delta z_{\rm A,max} t_{\rm pr}]\cos(2v_{\rm F}|k|(t - t_{\rm pr})) \\ & \times\Theta(t - t_{\rm pr}) + \frac{2i|z_k|}{z_k}\ {\rm Im}[(\delta z_{\rm A,max} t_{\rm pr}) p_s^*(\vec{k},t_{\rm pr})] \\ & \times \sin(2v_{\rm F}|k|(t_{\rm pr} - t))\Theta(t - t_{\rm pr}),\end{aligned}$$

where $\Theta(x)$ is the Heaviside's step function. We now work with the Fourier transformed probe polarization $\delta p(\omega') \equiv \sum_{\vec{k}} \delta p(\vec{k},\omega')$. Using this we may define the probe susceptibility as $\delta p(\omega') = \chi(\omega')\delta E(\omega')$, where $\delta E(\omega')$ is the electric field of the probe. Extracting $\chi(\omega')$ from the above equation and retaining only the most singular part we have, $\chi(\omega') \sim \cos\Phi(t_{\rm pr})$. We may see that the probe susceptibility depends on the area of pump pulse and it has oscillatory behaviour as a function of the duration of the pump field. After some simplification, we get the following expression:

$$\frac{\chi(\omega')}{\chi_{\rm max}(\omega')} = \cos(\Phi), \qquad \Phi = \frac{v_{\rm F}^2}{\hbar^2\omega^3}|\vec{\sigma}_{\rm BA}\cdot e\vec{E}_{\rm max}|^2(T_f - T_i). \tag{1}$$

Here we have restored Planck's constant to facilitate experimental verification of our central claim viz. eq. (1). Also, $\chi_{\rm max}(\omega')$ is the susceptibility when $\cos(\Phi) = 1$. The central result of eq. (1) may be depicted graphically as shown by the diagram in the results section.

4.2 *Differential transmission coefficient*

The above description was an ideal pump–probe experiment where the probe duration is taken to be much smaller than the pump duration, so much so that we have used an ideal delta function in time to describe the probe. This enables an elegant analytical solution of the probe susceptibility at each probe frequency. This solution also clearly and easily brings out the important physics we seek, viz., that the probe susceptibility is a sinusoidal function of the pump duration with the probe frequency and the pump Rabi frequency (electric field strength) remaining fixed. The period of these oscillations is the anomalous Rabi frequency. Realistic experiments [17–20] typically use the same pulse for pump and probe, except that the probe beam is much less intense than the pump and comes after a time delay following the pump. Therefore, in order to compare with the existing experimental data we wish to study this problem. When delays are present, it is important to take into account dephasing rates. To this end we write the pump equations as

$$\frac{\partial}{\partial t} n_{\rm diff}(\vec{k},t) = 4\ {\rm Im}[v_{\rm F}\vec{\sigma}_{\rm AB}\cdot\left(\vec{k}-\frac{e}{c}\vec{A}^*(t)\right)p(\vec{k},t)] \tag{2}$$

$$i\frac{\partial}{\partial t}p(\vec{k},t) = v_{\rm F}\vec{\sigma}_{\rm BA}\cdot\left(\vec{k}-\frac{e}{c}\vec{A}(t)\right)n_{\rm diff}(\vec{k},t) - i\frac{p(\vec{k},t)-p_0(\vec{k})}{T_2}. \tag{3}$$

Here $1/T_2$ is the polarization dephasing rate and $p_0(\vec{k}) = -z_k^*/2v_{\rm F}|k|$ is the equilibrium polarization. The above equation ensures that the polarization decays to the equilibrium value after a time which is much larger than T_2 once the pump is turned off. The probe equations become

$$\frac{\partial}{\partial t}\delta n_{\rm diff}(\vec{k},t) = 4\ {\rm Im}\left[v_{\rm F}\vec{\sigma}_{\rm AB}\cdot\left(-\frac{e}{c}\delta\vec{A}^*(t)\right)\ p(\vec{k},t)\right] + 4\ {\rm Im}[v_{\rm F}\vec{\sigma}_{\rm AB}\cdot\vec{k}\delta p(\vec{k},t)] \tag{4}$$

$$i\frac{\partial}{\partial t}\delta p(\vec{k},t) = v_{\rm F}\vec{\sigma}_{\rm BA}\cdot\left(-\frac{e}{c}\delta\vec{A}(t)\right)n_{\rm diff}(\vec{k},t) + v_{\rm F}\vec{\sigma}_{\rm BA}\cdot\vec{k}\delta n_{\rm diff}(\vec{k},t) - i\frac{\delta p(\vec{k},t)}{T_2}. \tag{5}$$

We have solved these equations using the methods already outlined to obtain the following formulas for transmission coefficient. In graphene we think of the induced field as proportional to the induced current, which is in turn proportional to the polarization. Therefore, we choose the contribution to the signal induced by the probe field as

$$\delta\vec{\pi}(t) = v_{\rm F}\vec{\sigma}_{\rm AB}\ \delta p(t) + v_{\rm F}\vec{\sigma}_{\rm BA}\delta p^*(t),$$

where $\delta p(t) = \frac{1}{A}\sum_{\mathbf{k}}\delta p(\mathbf{k},t)$. The signal due to the probe only is chosen for dimensional consistency as $\delta\vec{\pi}_{\rm ext}(t) = (ev_{\rm F}^2/c^2)\delta\mathbf{E}_{\rm ext}(t)$. The net transmitted signal is

$$\delta\vec{\pi}_{\rm trans}(t) = \delta\vec{\pi}_{\rm ind}(t) + \delta\vec{\pi}_{\rm ext}(t),$$

where $\delta\vec{\pi}_{\rm ind}(t)$ is the induced signal that propagates in the same direction as $\delta\vec{\pi}_{\rm ext}(t)$. The transmitted intensity is $\langle\delta\vec{\pi}^*_{\rm trans}(t)\cdot\delta\vec{\pi}_{\rm trans}(t)\rangle$ where the average denotes time average and the incident intensity is $\langle\delta\vec{\pi}^*_{\rm ext}(t)\cdot\delta\vec{\pi}_{\rm ext}(t)\rangle$. The transmission coefficient is,

$$\frac{\Delta T}{T_0} = \frac{\langle\delta\vec{\pi}^*_{\rm trans}(t)\cdot\delta\vec{\pi}_{\rm trans}(t)\rangle}{\langle\delta\vec{\pi}^*_{\rm ext}(t)\cdot\delta\vec{\pi}_{\rm ext}(t)\rangle}.$$

What we are really interested is the change in this coefficient with and without the pump. This means we have to calculate $(\Delta T_+ - \Delta T)/T_0$, where ΔT_+ refers to the probe transmission with the pump and ΔT is the same without the pump. In the present case, the induced signal is much weaker than the incident probe signal (it is well known that graphene is quite transparent (∼97%)). Hence we may write for the differential transmission coefficient

$$\eta \equiv \frac{\Delta T_+ - \Delta T}{T_0}$$

$$= \frac{\langle \delta\vec{\pi}^*_{\rm ext}(t) \cdot (\delta\vec{\pi}_{\rm ind,+}(t) - \delta\vec{\pi}_{\rm ind}(t))\rangle + \langle (\delta\vec{\pi}^*_{\rm ind,+}(t) - \delta\vec{\pi}^*_{\rm ind}(t)) \cdot \delta\vec{\pi}_{\rm ext}(t)\rangle}{\langle \delta\vec{\pi}^*_{\rm ext}(t) \cdot \delta\vec{\pi}_{\rm ext}(t)\rangle}.$$

We have computed η explicitly and it may be written as

$$\eta = -\frac{ic^2}{\omega^2 A} \sum_{\mathbf{k}} \mathrm{e}^{\lambda_2 \tau} \frac{1}{\tau_{\rm d}} \frac{(\mathrm{e}^{\lambda_2 \tau_{\rm d}} - 1)^2}{\Omega_{\rm ARWA}(0)} + \text{c.c.}, \tag{6}$$

where

$$\lambda_2 = -\frac{1}{2T_2} - \frac{\Omega^2_{\rm ARWA}(0)}{2T_2 \Omega^2_{\rm ARWA}(k)} - i\Omega_{\rm ARWA}(k) \tag{7}$$

and $\Omega_{\rm ARWA}(k)$ is the effective anomalous Rabi frequency and τ is the time delay between the end of the pump pulse and start of the probe pulse. Also $\tau_{\rm d}$ is the common duration of the pump and probe pulses. This may be explicitly evaluated for graphene to yield

$$\begin{aligned}\eta \;=\; & -\frac{c^2}{(4\pi v_{\rm F}^2(\tau + \tau_{\rm d})(\tau + 2\tau_{\rm d})\omega^2)} \\ & \times \Bigg(\left(4 + \frac{2\tau}{\tau_{\rm d}}\right) \cos\left[(\tau + \tau_{\rm d})\frac{2\omega_{\rm R}^2}{\omega}\right] \mathrm{e}^{-(\tau+\tau_{\rm d})/T_2} \\ & -\frac{(\tau + \tau_{\rm d})}{\tau_{\rm d}} \cos\left[\frac{2\omega_{\rm R}^2}{\omega}(\tau + 2\tau_{\rm d})\right] \mathrm{e}^{-(\tau+2\tau_{\rm d})/T_2} \\ & + \left(-3 - \frac{\tau}{\tau_{\rm d}} - \frac{2\tau_{\rm d}}{\tau}\right) \cos\left[\frac{2\omega_{\rm R}^2}{\omega}\tau\right] \mathrm{e}^{-\tau/T_2} \Bigg).\end{aligned} \tag{8}$$

It is clear from the above formula (consistent with the claims of the earlier discussion that involved using a delta function probe) that the susceptibility is a sinusoidal function of the pulse duration. Here, however, some differences are expected as both the pump pulse and the probe pulse have the same duration which means harmonics of anomalous Rabi frequency are also seen as a term such as $\cos[\frac{2\omega_{\rm R}^2}{\omega}(\tau_{\rm d,probe} + \tau_{\rm d,pump})]$ also appears, which in the earlier discussion was simply reduced to $\cos[\frac{2\omega_{\rm R}^2}{\omega}\tau_{\rm d}]$ as $\tau_{\rm d,probe} = 0$, but here as $\tau_{\rm d,probe} = \tau_{\rm d,pump} = \tau_{\rm d}$ there are harmonics as well. In this case, $T_2 \gg \tau \gg \tau_{\rm d}$. If we also ensure that $(2\omega_{\rm R}^2/\omega)\tau \sim 10$ so that there are about 10 anomalous Rabi oscillations

in the duration between pump and probe, this phenomenon is seen clearly in the periodic variation of the differential transmission coefficient as a function of delay. This formula also shows good agreement with experimental data [17–20]. Specifically, in the work of Breusing *et al* [18], a 7 fs pump and probe pulse was used with a pump fluence of 0.2 mJ/cm^2 corresponding to an intensity of $I_0 = 2.857 \times 10^{14}$ W/m^2 and the r.m.s. electric field corresponding to this intensity is $E = 3270.0$ kV/cm. The central frequency of the pump corresponds to $\hbar\omega = 1.5$ eV and the polarization dephasing time is taken to be $T_2 = 140$ fs. This leads to the following realistic values for the various frequency scales. The driving frequency is $\omega = 2.27 \times 10^{15}$ rad/s, the conventional Rabi frequency is $\omega_R = 2.19 \times 10^{14}$ rad/s and the anomalous Rabi frequency is $\Omega_{ARWA} = 2\omega_R^2/\omega = 4.2 \times 10^{13}$ rad/s. This means that in the duration of each pulse there are ∼16 oscillations with frequency ω, making this notion well defined. Also within the decay time there are ∼6 anomalous Rabi oscillations, making this also easily detectable. We may see that these numbers are completely consistent with the assumptions made in the asymptotic rotating wave approximation – each differs from the other by an order of magnitude or more. Now we wish to plot the theoretical analogue (see figure 1) of the data shown in figure 1c of Breusing *et al* [18].

In that work we see the following important features. The change in transmission is positive for time delays $\tau < 300$ fs and negative thereafter. The datapoints show oscillatory behaviour superimposed on an overall decay. We claim that this oscillatory behaviour is nothing but the anomalous Rabi oscillation. Indeed, an estimation of the period of these oscillations from figure 1c of Breusing *et al* gives a period of 107 fs. This corresponds to a circular frequency of 5.8×10^{13} rad/s, which is rather close to the anomalous Rabi frequency $\Omega_{ARWA} = 4.2 \times 10^{13}$ rad/s. Other features of this plot (figure 1c of Breusing *et al*) that are in broad agreement with eq. (8) are: (a) in both these plots, there is a sharp drop in the magnitude with increasing delays especially for small delays, (b) in both these plots, there is the all-important oscillation superimposed on this decay whose frequencies are in good agreement – a signature of anomalous Rabi oscillation and (c) both change sign after a certain time delay (however, the numerical values of those times do not match, also the numerical values of the coefficient do not match at all, ours is a bit too high).

The important point is that the oscillatory behaviour is characteristic, robust and common to both theory and experiment.

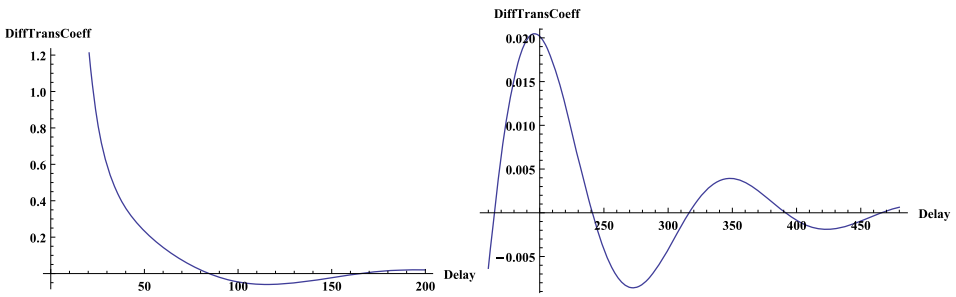

Figure 1. These figures depicts the variation of differential transmission coefficient vs. the time duration between the pump and probe fields.

4.3 *Linear response of bilayer*

To linearize the Bloch equations for bilayer make the substitution

$$n_{\text{diff}}(\vec{k},t) = n_s(\vec{k},t) + \delta n(\vec{k},t), \qquad p(\vec{k},t) = p_s(\vec{k},t) + \delta p(\vec{k},t)$$

and

$$A(t) \to A(t) + \delta A(t).$$

The linearized Bloch equations (keeping in mind that pump and probe are not present together, $A(t)\times\delta A(t) \equiv 0$) may be written in the frequency domain using a delta function probe $\delta A(t) = \delta A(t_{\text{pr}})\delta(t - t_{\text{pr}})$ as follows:

$$\omega'\delta n(\vec{k},\omega') = -\frac{1}{m}\left(2i\ \text{Im}[k_-^2\delta p(\vec{k},\omega')] - Q(\vec{k},t_{\text{pr}})\right)$$

$$\omega'\delta p(\vec{k},\omega') = -\frac{1}{2m}\left(k_+^2\delta n(\vec{k},\omega') - 2\frac{e}{c}k_+\delta A(t_{\text{pr}})n_s(\vec{k},t_{\text{pr}})\right)$$

$$Q(\vec{k},t_{\text{pr}}) = 4i\frac{e}{c}\text{Im}[k_-\ \delta A^*(t_{\text{pr}})p_s(\vec{k},t_{\text{pr}})],$$

where

$$p_s(\vec{k},t_{\text{pr}}) = \frac{k_+^2}{2|k|^2}\left(\cos\Phi + i\frac{\omega\Omega_{\text{AR}}}{\omega_{\text{R}}^2}\sin\Phi\right)$$

and

$$n_s(\vec{k},t_{\text{pr}}) = \frac{\omega|k|^2}{2m\omega_{\text{R}}^2(\bar{t})}\ \cos\Phi(t_{\text{pr}}).$$

Here Φ is the area of the pulse for the pump field given by (we assume that the system is probed immediately at the end of the pump pulse),

$$\Phi(t_{\text{pr}}) = \int_{T_i}^{t_{\text{pr}}} 2\Omega_{\text{AR}}(t)\text{d}t = \frac{1}{3\omega}\left(\frac{1}{2m}\right)^2\left(\frac{e}{c}\right)^4|A(0)|^4(T_f - T_i)$$

$$= \frac{2\omega_{\text{R}}^2}{\omega}(T_f - T_i).$$

The current induced by the probe is given by $\delta J(\omega') = \sum_{\vec{k}} k_-\delta p(\vec{k},\omega')$. The probe susceptibility is defined by the relation $\delta J(\omega') = \delta\chi(\omega')\delta E(\omega')$. Following a procedure similar to the single-layer case we may write

$$\delta\chi(\omega') \sim \cos\Phi(t_{\text{pr}}).$$

Thus we can see that the probe susceptibility depends on the time duration of the pulse field and oscillates with the anomalous Rabi frequency $2\omega_{\text{R}}^2/\omega$ as a function of this duration.

4.4 *Linear response of multilayer*

To linearize the Bloch equation for multilayer graphene we use similar procedure as in the case of single layer and bilayer. In presence of probe field taken as a delta function, $(\delta A(t) = \delta A(t_{\rm pr})\delta(t - t_{\rm pr}))$, the linearized Bloch equation is given by

$$i\frac{\partial}{\partial t}\delta N_\nu(\vec{k}, t) = 4\beta\ \mathrm{Im}\Big(k_-^n \delta\pi_\nu(\vec{k}, t) - n\frac{e}{c}\, k_-^{(n-1)}\delta A(t_{\rm pr})\pi_\nu(\vec{k}, t_{\rm pr})\Big)\delta(t - t_{\rm pr}),$$

$$i\frac{\partial}{\partial t}\delta\pi_\nu(\vec{k}, t) = \beta\Big(k_+^n\ \delta N_\nu(\vec{k}, t) - n\ \frac{e}{c}\ k_+^{(n-1)}\delta A(t_{\rm pr})N_\nu(\vec{k}, t_{\rm pr})\Big)\delta(t - t_{\rm pr}).$$

The multilayer case is entirely analogous to the single and bilayer cases already discussed. After straightforward calculations, quote the final results. In the case of multilayer graphene, the area of the pump pulse $\Phi(t)$ is given by

$$\Phi(t_{\rm pr}) = \frac{2\omega_{\rm R}^2}{\omega}(T_f - T_i),$$

where $T_f - T_i$ is the pump pulse duration and

$$\omega_{\rm R}^2 = \beta^2\frac{1}{n}\left(\frac{e}{c}\right)^{2n}|A(0)|^{2n}$$

is the square of the conventional Rabi frequency of multilayer graphene and $\beta = v_{\rm F}^n/\gamma_1^{n-1}$ is the prefactor that appears in Hamiltonian of multilayer graphene. As before, the probe susceptibility is $\chi(\omega') \sim \cos\Phi(t_{\rm pr})$.

5. Results and discussion

In this section, we plot a graph obtained from eq. (1), which reveals that the susceptibility due to the probe field depends on the area of the pump pulse. This area is proportional to the pump pulse duration $(T_f - T_i)$, provided the conventional Rabi frequency is held fixed. The frequency of oscillations of the probe susceptibility as a function of pump pulse duration is just the anomalous Rabi frequency (figure 2).

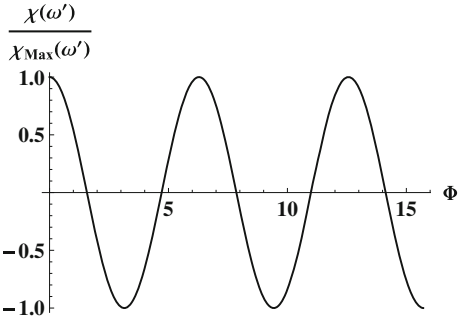

Figure 2. The above plot of eq. (1) depicts the variation of probe susceptibility with the area of the pump pulse.

Alternatively, graphene mimicked using cold atoms [28] could also be a possibility where such constraints may be circumvented as the experiments can be tailor-made to a theory's specifications. The surface states of a three-dimensional topological insulator are also Dirac fermions [29], but they possess conventional spin rather than pseudospin. The analysis of the present work shows that in such systems too (gapped or without gap) anomalous Rabi oscillations are seen.

6. Conclusions

In this work, we have shown how pump–probe experiments can detect anomalous Rabi oscillations in graphene and graphene-like systems such as surface states of topological insulators. Anomalous Rabi oscillations are like conventional Rabi oscillations – periodic exchange of energy between the light field and the system in question. However, instead of these oscillations taking place close to the resonance criterion, where the applied frequency is nearly equal to the frequency for creating a particle–hole pair, anomalous Rabi oscillations are seen when the external frequency is larger than all other frequencies present in the system. We have shown that these anomalous oscillations have a frequency equal to $2\omega_{\mathrm{R}}^2/\omega$ where ω_{R} is the conventional Rabi frequency and ω is the applied frequency. These anomalous oscillations were shown in an earlier work to be solely due to pseudospin/conventional spin, Dirac–fermion nature of the quasiparticles. These qualities are shared by both the graphene system and topological insulators. These anomalous oscillations manifest themselves in the pump–probe experiment as a periodic variation of the probe susceptibility which is a function of pump duration when the conventional Rabi frequency is held fixed.

7. Author's contribution

SLG pump–probe calculations, BLG and MLG probe calculations and some literature survey were done by Enamullah, pump result calculation for BLG and MLG was performed by Vipin Kumar, literature survey and verification of calculations were done by Upendra Kumar and the differential transmission calculation, general guidance on the way to do the calculations and writing the manuscript were done by Dr Girish S Setlur.

References

[1] K S Novoselov, A K Geim, S V Morozov, D Jiang, Y Zhang, S V Dubonos, I V Grigorieva, and A A Firsov, *Science* **306**, 666 (2004)
[2] A H Castro Neto, F Guinea, N M R Peres, K S Novoselov and A K Geim, *Rev. Mod. Phys.* **81**, 109 (2009)
[3] P R Wallace, *Phys. Rev.* **71**, 622 (1947)
[4] E McCann, D S L Abergel and V I Fal'ko, *Eur. Phys. J. Special Topics* **148**, 91 (2007)
[5] M Mucha-Kruczynski, E McCann and V I Fal'ko, *Semicond. Sci. Technol.* **25**, 033001 (2010)
[6] Enamullah, Vipin Kumar and Girish S Setlur, *Physica B* **407**, 4600 (2012)
[7] I I Rabi, *Phys. Rev.* **51**, 652 (1937)

[8] L Allen and J H Eberly, *Optical resonances and two-level atoms* (Wiley and Sons, New York, 1975)
[9] H Haug and S W Koch, *Quantum theory of optical and electronic properties of semiconductors*, Fourth Edition (World Scientific, 2004)
[10] D Frohlich, A Nothe and K Reimann, *Phys. Rev. Lett.* **55**, 1335 (1985)
[11] S Schmitt-Rink, D S Chemla and H Haug, *Phys. Rev. B* **37**, 941 (1988)
[12] C Ell, J F Muller, K El Sayed and H Haug, *Phys. Rev. Lett.* **62**, 304 (1989)
[13] J Shang, Z Luo, C Cong, J Lin, T Yu and G G Gurzadyan, *Appl. Phys. Lett.* **97**, 163103 (2010)
[14] P A George, J Strait, J Dawlaty, S Shivaraman, M Chandrashekhar, F Rana and M G Spencer, *Nano Lett.* **8**, 4248 (2008)
[15] D Sun, Zong-Kwei Wu, C Divin, X Li, C Berger, W A de Heer, P N First and T B Norris, *Phys. Rev. Lett.* **101**, 157402 (2008)
[16] B A Ruzicka, L K Werake, H Zhao, S Wang and K P Loh, *Appl. Phys. Lett.* **96**, 173106 (2010)
[17] J M Dawlaty, S Shivaramam, M Chandrashekhar, F Rana and M G Spencer, *Appl. Phys. Lett.* **92**, 042116 (2008)
[18] M Breusing, S Kuehn, T Winzer, E Malic, F Milde, N Severin, J P Rabe, C Ropers, A Knorr and T Elsaesser, *Phys. Rev. B* **83**, 153410 (2011)
[19] S Kumar, M Anija, N Kamaraju, K S Vasu, K S Subrahmanyam, A K Sood and C N R Rao, *Appl. Phys. Lett.* **95**, 191911 (2009)
[20] S Kumar, N Kamaraju, K S Vasu, A Nag, A K Sood and C N R Rao, *Chem. Phys. Lett.* **499**, 152 (2010)
[21] H Wang, J H Strait, P A George, S Shivaraman, V B Shields *et al*, *Appl. Phys. Lett.* **96**, 081917 (2010)
[22] R Ulbricht, E Hendry, J Shan, T F Heinz and M Bonn, *Rev. Mod. Phys.* **83**, 543 (2011)
[23] Q Chen *et al*, *Scientific Reports* **3**(2315) (2013), DOI:10.1038/srep02315
[24] A Das *et al*, *Nature Nanotechnol.* **3**, 210 (2008)
[25] M Farkas, *Applied mathematical science 104: Periodic motions* (Springer, New York, 2010)
[26] S R Barone and M A Narcowich, *Phys. Rev. A* **15**, 1109 (1977)
[27] F Zhang, B Sahu, H Min and A H MacDonald, *Phys. Rev. B* **82**, 035409 (2010)
[28] L Tarruell, D Greif, T Uehlinger, G Jotzu and T Esslinger, *Nature* **483**, 302 (2012)
[29] D Hsieh, D Qian, L Wray, Y Xia, Y S Hor, R J Cava and M Z Hasan, *Nature (London)* **452**, 970 (2008)
D Hsieh, Y Xia, L Wray, D Qian, A Pal, J H Dil, J Osterwalder, F Meier, G Bihlmayer, C L Kane, Y S Hor, R J Cava and M Z Hasan, *Science* **323**, 919 (2009)